Design of a compliant positioning control using an inverse method

Eric Bideaux, Mohamed Smaoui, Xavier Brun, Daniel Thomasset

DESIGN OF A COMPLIANT POSITIONNING CONTROL USING AN INVERSE METHOD

Eric BIDEAUX, Mohamed SMAOUI, Xavier BRUN, Daniel THOMASSET

Laboratoire d'Automatique Industrielle, INSA Lyon, Bâtiment Saint Exupéry,25 Avenue Jean Capelle, 69621 Villeurbanne Cedex, France, http://csiges7.insa-lyon.fr/lai/lai_gb.html
Email: eric.bideaux@lai.insa-lyon.fr

Abstract: The design of new system requires generally achieving different objectives. The choice of the right system and control architecture is crucial and they can be judiciously exploited. The proposed approach is dealing with the efficient use of a pneumatic cylinder controlled by two servovalves. The control objectives are independent position and stiffness tracking. A Bond graph approach gives, in a first step, a general methodology to check the accessibility of the specifications on energetic and dynamic criteria. Then a control algorithm issued from the flatness concept and the nonlinear control theory is developed. Simulation and experimental results illustrating the proposed principle are finally presented. Concerning the tracking performance, it is shown that the new strategy does not decrease tracking errors, or the static errors, or the standard deviation in term of position and velocity tracking. The performance of the stiffness control is finally illustrated in simulation.

Keywords: Electropneumatic, inverse method, Bond graph, nonlinear control, flatness.

NOMENCLATURE

a	acceleration (m/s^2)
A	area of thermal exchange (m^2)
b	viscous coefficient (N/m/s)
c_P	heat transfer coefficient at constant pressure (J/kg/K)
c_v	heat transfer coefficient at constant volume (J/kg/K)
F	force (N)
h	enthalpy per mass unit (J/s/kg)
j	jerk (m/s^3)
k	polytropic constant
K	stiffness (N/m)
K_{th}	convection coefficient (W/K/m^2)
m	mass of gas (kg)
M	moving load (kg)
P	pressure (Pa)
q_m	mass flow rate (kg/s)
dQ/dt	convection heat transfer (J/s)
r	perfect gas constant (J/kg/K)
S	area of the piston cylinder (m^2)
t	time (s)
T	temperature (K)
u	servo-distributor input voltage (V)
U	internal energy (J)
v	velocity (m/s)
V	volume (m^3)
x	state vector
y	position (m)
λ	feedback gain
$\varphi(.)$, $\psi(.)$	are polynomial functions

Subscripts and superscripts

cyl	cylinder
d	desired
ext	external
E	exhaust
f	dry friction
N	chamber N
P	chamber P
S	supply

1 – Introduction

At the present time, five-way servovalves or servo-distributors are used to control many actuators for position or velocity tracking. The trend of building longer rodless cylinders is one of the principal reasons for the development of three-way electropneumatic modulators. In fact the integration of this component in each cylinder extremity reduces the congestion and the length of

the pneumatic pipes. The particular structure of this technology has not been very much exploited for control strategies. Indeed, the constructors usually use these two three-way modulators with the same air power supply and the same input controls but with opposite signs, which is equivalent to using one five-way servo-distributor.
Using two servo-distributors leads to a system with two degrees of freedom according to the control and this opportunity is exploited to achieve two different control objectives. Taking advantage of the supplementary degree of freedom issued from this new design, it is possible to control another output other than the position control. In a first study (1), the second design objective was to limit energy consumption in order to increase the pneumatic servodrive efficiency. In this new approach, the second objective is to control the pneumatic stiffness, which influences directly the system compliancy. Thus it is possible to respect two different objectives, with two dissociated controls.
This type of application shows the advantages of the use of inverse methods to determine the open loop control input according to the objective trajectory. The bicausality concept (2), which is related to the bond graph approach, allows checking the flatness of the outputs and also their structural properties. Finally, the desired output trajectories may be introduced in the bond graph model in order to determine the required open loop control input and also to show the existing physical limitations, which may appear. The general method using the bond graph approach is explained before being applied to the proposed problem.

2 – Flat outputs and inverse system study using Bond graph approach

As the Bond graph is an energy-based graphical language, it showed advantages in mechatronic system modelling and analysis (3). One of the main interests of the Bond graph approach is to propose by the way of the causality concept a graphical tool for the study of structural analysis and engineering problem solvability. This last point has been recently extended to design problems with the help of the bicausality concept, which gives a straightforward solution for the graphical and analytical study of inverse problems, that is to say most of the design problems.

2.1 – Inverse system and Bond graph

The bicausality concept introduced implicitly by Cornet and Lorenz (4) and more formally by Gawthrop (2), has introduced a new philosophy in regards to a bond graph model. It allows to force the value of the power by imposing effort and flow on a bond. This approach has to be related to a mathematical research in an oriented graph. In one hand, "standard" causality, the imposed variable on a bond is either the effort, or the flow variable. It is then a physical way to give an orientation to the acausal relations characterising each elementary phenomenon. The result is the identification of the numerical difficulties (dependencies, algebraic loops, etc) and the mathematical model to be solved within simulation tools. In the other hand, the bicausality concept introduces mathematical orientations of the constitutive relations of the phenomena, which have no more physical meaning. But the result is still a mathematical model and a graphical tool to identify the numerical difficulties. The bicausality allows to fix or impose a variable and its conjugate at the same time since bicausal bonds decouple the effort and flow causalities. The meaning of this statement is that it is assumed that the behaviours of the flow and the effort is known or imposed at a specific place in the system, and this approach allows the study of some kind of inverse problems. This principle has been successfully applied in design or sizing problem (5, 6, 7) and in control synthesis (8).
In the context of design problems, the specifications give usually the performance to reach in terms of output trajectories. The problem is then to determine the structure, the parameters of the system

and its inputs, which permit to reach the design requirements. This constitutes clearly an inverse problem. Imposing the outputs (or the trajectory issued from design specifications) without modifying the system structure can be carried out with an SS element which has a flow source / effort source causality. To indicate the desired outputs and let the structure of the system show by itself the required power and input signals, one the power variable of the SeSf element is set to the desired trajectory while the conjugate variable is set to a null value. This leads to a null power flow on that bond but constraints the system behaviour. Similarly, the input variable of the system to be determined will be detected on a DeDf element with a flow sensor / effort sensor causality. The MSCAPI procedure (9) allows to complete the causality assignment in the Bond graph and the results may be used to identify the physical, the numerical difficulties, and to determine the inverse model.
The bicausality concept may be used to directly determinate either the control law to apply to the system or a physical parameter in the system in order to obtain the desired trajectory. The control law is usually given by the modulation of an R-element, which is related to the power modulator of the system. The physical parameter may be any parameter in the system: GY, TF, R, I and C-type elements.

2.2 – System inversion using Bond graph methodology

Gawthrop (2, 8), N'Gwompo et al. (5, 6, 7, 9, 10), Scavarda, Marquis-Favre and Bideaux (11, 12) have proposed different approaches, uses and results for this kind of problems. A first procedure giving the condition of existence and allowing to determine the inverse has been proposed in the general case of non-linear MIMO systems:
1) Determine all the set of paths in between inputs and outputs on the Bond graph in integral causality,
Conclusion: if at least one set of independent paths does exist, the system is structurally inversible.
2) Compute the input-output path order, where the order of a path in the number of storage element in integral causality minus the number of storage element in derivative causality along the path.
Conclusion: the order of a path is corresponding to effective number of integration along the path.
3) Introduce the double sources SeSf and the double detector DeDf, and propagate the bicausality along the input-output paths using the set of independent paths of lowest order.
4) Complete the causality using the MSCAPI and in nonlinear cases, check the mathematical inversibility of each element constitutive relation.
Conclusion: if at least one complete causality assignment does exist, the system is mathematically inversible.

2.3 – Flat systems

In nonlinear control theory, the concept of flatness has opened new ways for the control synthesis of complex systems. In non linear control theory, the concept of flatness has opened new ways for the control synthesis of complex systems.
One of the classes of systems for which trajectory generation is particularly easy are so-called differentially flat systems (13). Roughly speaking, a system is differentially flat if we can find a set of outputs (equal in number to the number of inputs) such that all states and inputs can be determined from these outputs without integration. More precisely, if the system has states $x \in \Re^n$, and inputs $u \in \Re^m$ then the system is flat if it is possible to can find outputs $y \in \Re^m$ of the form $y = f_1\left(x, u, \dot{u}, ..., u^{(p)}\right)$, such that: $x = f_2\left(y, \dot{y}, ..., y^{(q)}\right)$ and $u = f_3\left(y, \dot{y}, ..., y^{(q+1)}\right)$

One of the main interests of searching a set of flat outputs is that the use of such a set allows decoupling and linearising the system outputs. By introducing for each input their expressions as function of the successive derivatives of the outputs (figure 1), the problem of the control synthesis becomes a classical problem of decoupled linear system control (14).
It appears clearly that the Bond Graph inversion procedure can be efficiently apply to determine if a set of outputs is or not flat.

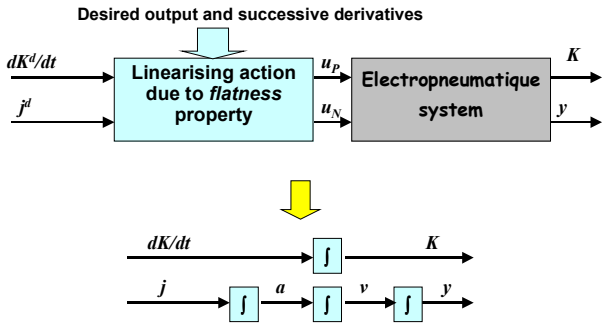

Figure 1: Flat system linearization

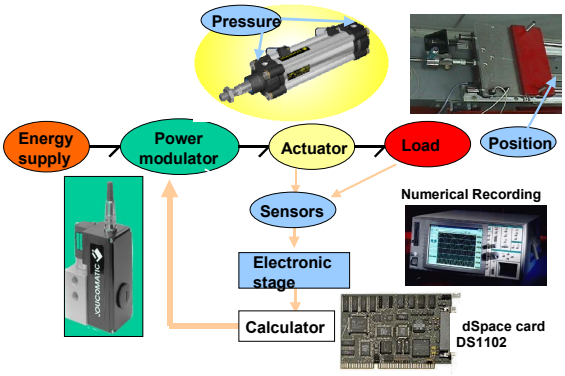

Figure 2: Experimental rig

2.4 – Application to the pneumatic cylinder

Our objective is here to show the methodology applied to the control in position and in stiffness of a pneumatic cylinder. In a first step, the Bond graph model is developed and the input-output paths are shown. The bicausal bond graph is then proposed and the inverse model determine. Finally the system control is developed and simulated results are shown. The difficulties are related here to the nonlinearity of the system and to the thermal behaviour modelling complexity. Therefore the methodology will be first applied to a more realistic model (simulation model) whereas a simpler model is used in a second step for the control synthesis (control model).

3 – Bond graph modelling

The experimental bench (figure 2) is an in-line electropneumatic servodrive controlled by two three-way servo-distributors. The stroke length is half a meter and the total moving load is 17 kg. The electropneumatic system model uses classical assumptions (15): by considering the pressure behavior in a chamber with variable volume and the mechanical equation which includes pressure force, viscous friction (bv), dry friction (F_f) and an external force (F_{ext}) due to atmospheric pressure. Using the theory of multi-scale systems, the dynamics of the servovalves can be neglected [4]. Then the model can be reduced to a static characteristic for given supply and exhaust pressures and is described by two relationships $q_{mP}(P_P, u_P)$ and $q_{mN}(P_N, u_N)$ between the mass flow rates q_{mP} and q_{mN}, the input voltages u_P and u_N, and the output pressures P_P and P_N.
The Bond graph model shown figure 3 uses the pseudo-bond graph approach for the pneumatic part. The two chambers are represented by the 3-ports C-elements, which constitutive relations are given by equations (2) and (3). Each orifice of the servovalve is represented by a 4-ports R element modulated by its respective input voltages u_P and u_N. The thermal exchange from the gas in each chamber and the cylinder is a dissipation phenomenon represented by an R-element according to the equation (4). Applying the integral causality to the acausal bond graph, the simulation model is the following.

Mechanical part:
$$\begin{cases} M\dfrac{dv}{dt} = S_P P_P - S_N P_N - bv - F_{ext} - F_f \\ \dfrac{dy}{dt} = v \end{cases} \quad (1)$$

Chamber N:
$$\begin{cases} \dfrac{dU_N}{dt} = q_{mSN} h_S - q_{mNE} h_N - P_N \dfrac{dV_N}{dt} + \dfrac{dQ_N}{dt} \\ \dfrac{dm_N}{dt} = q_{mSN} - q_{mNE} \\ \dfrac{dV_N}{dt} = -S_N v \end{cases} \text{ and } \begin{cases} P_N = \dfrac{r}{c_v}\dfrac{U_N}{V_N} \\ T_N = \dfrac{1}{c_v}\dfrac{U_N}{m_N} \end{cases} \quad (2)$$

Chamber P:
$$\begin{cases} \dfrac{dU_P}{dt} = q_{mSP} h_S - q_{mPE} h_P - P_P \dfrac{dV_P}{dt} + \dfrac{dQ_P}{dt} \\ \dfrac{dm_P}{dt} = q_{mSP} - q_{mPE} \\ \dfrac{dV_P}{dt} = S_p v \end{cases} \text{ and } \begin{cases} P_P = \dfrac{r}{c_v}\dfrac{U_P}{V_P} \\ T_P = \dfrac{1}{c_v}\dfrac{U_P}{m_P} \end{cases} \quad (3)$$

Thermal Exchange:
$$\frac{dQ_N}{dt} = K_{th} A_N(y)\left(T_{cyl} - T_N\right) \text{ and } \frac{dQ_P}{dt} = K_{th} A_P(y)\left(T_{cyl} - T_P\right) \quad (4)$$

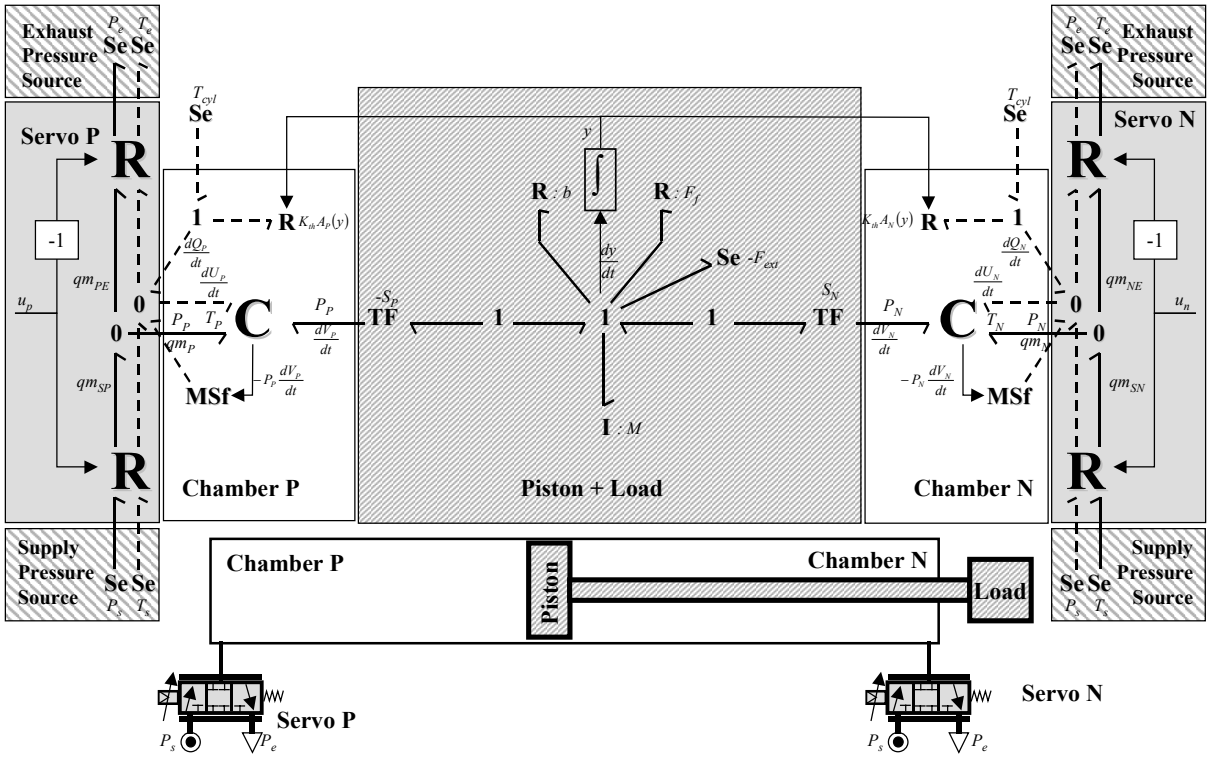

Figure 3: Bond graph model of the electropneumatic servodrive

As the servovalves characteristics are known for given exhaust and supply pressures, it is convenient to simplify the Bond graph using these global characteristics according to the figure 4.

The stiffness of the electropneumatic servodrive is given by equation (5) and is introduced on the Bond graph. In this system, many input-output paths may be determined but to check the structural inversibility of the system only independent paths are necessary. The two dot lines show the selected independent input-output paths showing the structural inversibility of the system for the given set of inputs (u_P, u_N) and outputs (K,y). The lengths of the paths are respectively 3 from u_N toward K, and 5 from u_P toward y. The sum of the path lengths is then 8 and is equal to the system dimension. Because of the physical symmetry of the system, a symmetrical choice of input-output paths can be done in which u_P is related to K and u_N to y.

$$K = k\left(\frac{S_N{}^2}{V_N}P_N + \frac{S_P{}^2}{V_P}P_P\right) \tag{5}$$

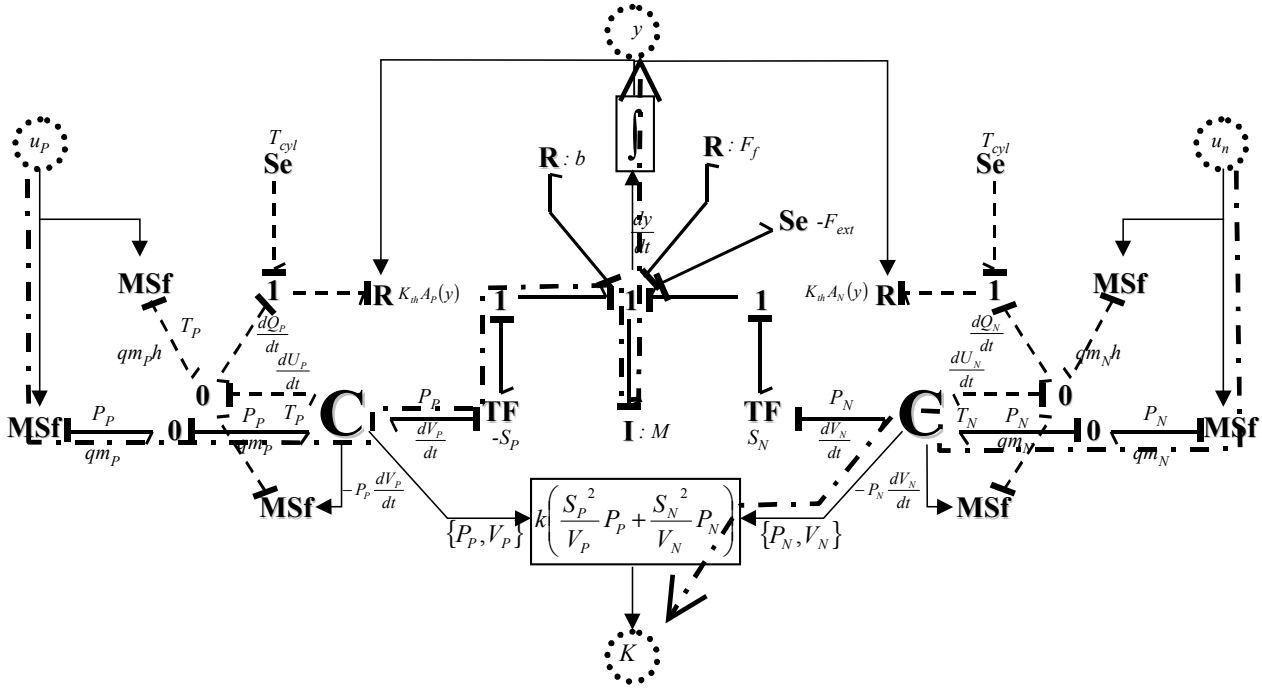

Figure 4: Simplified Bond graph model of the electropneumatic servodrive and input-output paths

4 – Model Inversion

As shown previously (figure 4), considering the stiffness as an output constitutes a problem because it is not directly linked to a power variable on the Bond graph. It is possible to consider that it can be equivalent to impose the pressure in one chamber if the position is imposed to the other chamber. Considering K(t), y(t) and their derivative known, the two pressures P_P and P_N can be expressed as functions of K(t), y(t) and their derivative according to resolution of the system (6), which corresponds, to the inversion of the mechanical part.

$$\begin{cases} M\dfrac{dv}{dt} - S_P P_P + S_N P_N + bv + F_{ext} + F_f = 0 \\ K - k\left(\dfrac{S_N{}^2}{V_N}P_N + \dfrac{S_P{}^2}{V_P}P_P\right) = 0 \end{cases} \tag{6}$$

$$\begin{cases} P_P = \dfrac{V_P(y)}{S_P}\dfrac{1}{S_N V_P(y) + S_P V_N(y)}\left[V_N(y)\dfrac{K}{k} + S_N\left(M\dfrac{d^2y}{dt^2} + b\dfrac{dy}{dt} + F_{ext} + F_f \right)\right] \\ P_N = \dfrac{V_N(y)}{S_N}\dfrac{1}{S_N V_P(y) + S_P V_N(y)}\left[V_P(y)\dfrac{K}{k} - S_P\left(M\dfrac{d^2y}{dt^2} + b\dfrac{dy}{dt} + F_{ext} + F_f \right)\right] \end{cases} \quad (7)$$

From (7) it can be deduced that the stiffness trajectory can be introduced on the Bond graph by imposing the pressure P_N in the chamber N. Equation (7) can also be used to check the physical validity of the desired trajectories. As the pressures P_N and P_P are physically limited by the exhaust and supply pressures, it can be concluded that there are limitations:

- for stiffness if the desired position trajectory is imposed,
- and for position trajectory if the desired stiffness is imposed.

On the bicausal Bond graph (figure 5) the two desired trajectory y and now P_N are introduced using two SeSf elements and the two mass flow rate source elements corresponding to each servo are replaced by double detectors DeDf. The bicausality is then propagated toward the inputs u_P and u_N on the previously determined input-output paths and the causality assignment is completed using the MSCAPI.

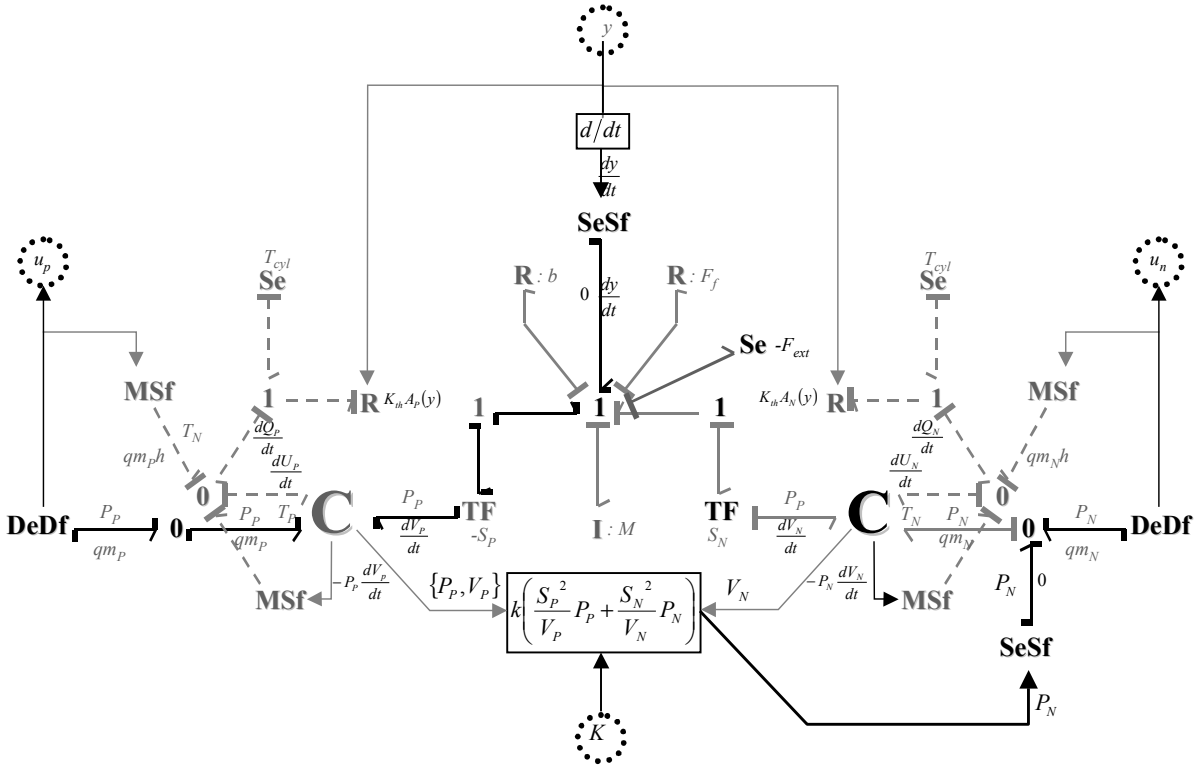

Figure 5: Bicausal Bond graph

All the storage elements are now in derivative causality, which means mathematically that integration in these elements, are yet replaced by differentiation of the imposed trajectory. With the help of equation (7) and because of the symmetric causality, the global problem may be reduced to two similar problems consisting in inversing the dynamic of each chamber. Equation (8) shows the numerical scheme for chamber N and the same result is obtained for chamber P.

$$\begin{cases} \dfrac{dU_N}{dt} = \dfrac{c_v}{r}\left(V_N(y)\dfrac{dP_N}{dt} + P_N \dfrac{dV_N}{dt} \right) \\ q_{mN} = \dfrac{dm_N}{dt} = \dfrac{1}{c_v}\left(\dfrac{1}{T_N}\dfrac{dU_N}{dt} - \dfrac{U_N}{{T_N}^2}\dfrac{dT_N}{dt} \right) \\ \dfrac{dV_N}{dt} = -S_N \dfrac{dy}{dt} \end{cases} \tag{8}$$

The causality in the rest of the system leads to the relation (9) and (10).

$$\frac{dQ_N}{dt} = \frac{dU_N}{dt} + P_N \frac{dV_N}{dt} - q_{mN} h \text{ with } \begin{cases} h = c_p T_N \text{ if } q_{mN} < 0 \\ h = c_p T_S \text{ if } q_{mN} \geq 0 \end{cases} \tag{9}$$

and $$T_N = \frac{1}{k_{th} A_N(y)} \frac{dQ_N}{dt} + T_{cyl} \tag{10}$$

Using equation (7) and substituting P_N and V_N by their expressions as a function of y, K and their derivative, the previous equations lead to the final relationship (11) in between q_{mN} and the desired trajectories y and K, and the successive derivative of these trajectories. The desired position has to be at least 5 times differentiable and the desired stiffness 3 times.

$$q_{mN} = g\left(y, \frac{dy}{dt}, \frac{d^2y}{dt^2}, \frac{d^3y}{dt^3}, \frac{d^4y}{dt^4}, \frac{d^5y}{dt^5}, K, \frac{dK}{dt}, \frac{d^2K}{dt^2}, \frac{d^3K}{dt^3} \right) \tag{11}$$

For control purposes and because the thermal effects are not well known in the cylinder, the model has to be simplified using a polytropic assumption concerning the thermodynamic behaviour of the gas. Equations (2) and (3) are then replaced by (12) and (13) where it is also assumed that the gas temperature stays closed to the room temperature T_S.

$$\frac{dP_N}{dt} = \frac{krT_S}{V_N}\left(q_{mSN} - q_{mNE} - \frac{P_N}{rT_S}\frac{dV_N}{dt} \right) \tag{12}$$

$$\frac{dP_P}{dt} = \frac{krT_S}{V_P}\left(q_{mSP} - q_{mPE} - \frac{P_P}{rT_S}\frac{dV_P}{dt} \right) \tag{13}$$

As previously, with the help of equation (7) and substituting P_N, P_P by their expressions as a function of y, K and their derivative, q_{mN} can be deduced from the knowledge of the desired trajectories y and K, and the successive derivative of these trajectories. Equations (14) and (15) give respectively the required mass flow rate for the servo N and the servo P, and at physical level, they are also useful to verify the size of the servovalves (16) according to the desired trajectories.

As the dimension of the system has been reduced to 4, the desired position has yet to be at least 3 times differentiable and the desired stiffness 1 time. As the static mass flow rate characteristic of the servovalves have been approximated by Belgharbi et al. (17) according to equation (16), the input voltages u_P and u_N can be deduced algebraically. It shows that the proposed outputs are flat because the inputs are functions of these outputs and of their derivative, and the sum of the characteristic indexes is equal to the system dimension. The nonlinear linearisation method may be applied using the calculated inverse model.

$$q_{mN} = \frac{1}{krT_S}\left(V_N(y)\frac{dP_N}{dt} + kP_N\frac{dV_N}{dt} \right)$$

$$= \frac{1}{krT_S}\frac{V_N(y)}{S_N}\frac{1}{S_N V_P(y) + S_P V_N(y)}\left[\begin{array}{l} \frac{K}{k}\frac{dy}{dt}\left(S_P V_N(y) - (k+1)S_N V_P(y)\right) + \frac{1}{k}V_P(y)V_N(y)\frac{dK}{dt} + \cdots \\ \cdots + S_N S_P(k+1)\frac{dy}{dt}\left(M\frac{d^2y}{dt^2} + b\frac{dy}{dt} + F_{ext} + F_f \right) + \cdots \\ \cdots - S_P V_N(y)\left(M\frac{d^3y}{dt^3} + b\frac{d^2y}{dt^2} + \frac{dF_f}{dt} \right) \end{array} \right] \quad (14)$$

$$q_{mP} = \frac{1}{krT_S}\left(V_P(y)\frac{dP_P}{dt} + kP_P\frac{dV_P}{dt} \right)$$

$$= \frac{1}{krT_S}\frac{V_P(y)}{S_P}\frac{1}{S_N V_P(y) + S_P V_N(y)}\left[\begin{array}{l} -\frac{K}{k}\frac{dy}{dt}\left(S_N V_P(y) - (k+1)S_P V_N(y)\right) + \frac{1}{k}V_P(y)V_N(y)\frac{dK}{dt} + \cdots \\ \cdots + S_N S_P(k+1)\frac{dy}{dt}\left(M\frac{d^2y}{dt^2} + b\frac{dy}{dt} + F_{ext} + F_f \right) + \cdots \\ \cdots - S_N V_P(y)\left(M\frac{d^3y}{dt^3} + b\frac{d^2y}{dt^2} + \frac{dF_f}{dt} \right) \end{array} \right] \quad (15)$$

$$q_{mP}(P_P, u_P) = \varphi(P_P) + \psi(P_P, sgn(u_P))u_P \text{ and } q_{mN}(P_N, u_N) = \varphi(P_N) + \psi(P_N, sgn(u_N))u_N \quad (16)$$

This part as shown that it is possible by applying the proposed methodology for system inversion to obtain crucial information concerning the capacity of the system to achieve the required task but also to determine interesting properties for nonlinear control purposes:

- Physical limitations of the desired trajectories (range of pressures),
- Mathematical properties of the trajectories (differentiability),
- Size of the power modulator (mass flow rate limitations),
- Flatness of the outputs.

5 – Control synthesis

In this part, the classical method issued from nonlinear control theory is applied to show the flatness of the output, and then to synthesize the control law implemented. Finally simulation results are presented. The model used for control synthesis is given by equation (17) and is corresponding to the simplified case used for system inversion (section 4).

$$\left\{ \begin{array}{l} \frac{dy}{dt} = v \\ \frac{dv}{dt} = \frac{1}{M}\left[S_P p_P - S_N p_N - bv - F_{ext} \right] \\ \frac{dp_P}{dt} = \frac{krT_s}{V_P(y)}\left[\varphi(p_P) - \frac{S_P}{rT_s}p_P v \right] + \frac{krT_s}{V_P(y)}\psi(p_P, sgn(u_P))u_P \\ \frac{dp_N}{dt} = \frac{krT_s}{V_N(y)}\left[\varphi(p_N) + \frac{S_N}{rT_s}p_N v \right] + \frac{krT_s}{V_N(y)}\psi(p_N, sgn(u_N))u_N \end{array} \right. \quad (17)$$

Let's define $h(\underline{x})$ the vector constituted of the two chosen outputs: position and stiffness:

$$h(\underline{x}) = \begin{pmatrix} h_1(\underline{x}) \\ h_2(\underline{x}) \end{pmatrix} = \begin{pmatrix} y \\ k\left[\frac{S_p^2 P_P}{V_p(y)} + \frac{S_N^2 P_N}{V_N(y)}\right] \end{pmatrix} \tag{18}$$

The characteristic number associated to the position and the stiffness are, respectively, three and one. Thus, the sum is equal to the dimension of the system. This is sufficient to affirm that the system is differentially flat. According to flatness definition (section 2.3) and figure 1, the model can be transformed into:

$$\begin{cases} \frac{d^3 y}{dt} = w_2 \\ \frac{dK}{dt} = w_1 \end{cases} \tag{19}$$

Then the control inputs (20) is obtained by inversion of the model (18),

$$u_P = \frac{1}{\frac{krT_S}{M}\frac{S_p}{V_p(y)}\psi(p_P, sgn(u_p))}\left[\frac{w_1 - f(y,v,p_P,p_N)}{kM\left[\frac{Sp}{V_p(y)} + \frac{S_N}{V_N(y)}\right]} + \frac{w_2 - h(y,v,p_P,p_N)}{1 + \frac{S_P V_N(y)}{S_N V_P(y)}}\right]$$

$$u_N = \frac{-1}{\frac{krT_S}{M}\frac{S_N}{V_N(y)}\psi(p_N, sgn(u_N))}\left[\frac{-(w_1 - f(y,v,p_P,p_N))}{kM\left[\frac{Sp}{V_p(y)} + \frac{S_N}{V_N(y)}\right]} + \frac{w_2 - h(y,v,p_P,p_N)}{1 + \frac{S_N V_P(y)}{S_P V_N(y)}}\right] \tag{20}$$

where

$$h(y,v,p_P,p_N) = \frac{krT_s}{M}\left(\frac{S_p}{V_p(y)}\varphi(p_p) - \frac{S_N}{V_N(y)}\varphi(p_N) - \frac{v}{rT_s}\left(\frac{S_p^2 p_P}{V_P(y)} + \frac{S_N^2 p_N}{V_N(y)}\right)\right) - \frac{b}{M^2}(S_P p_P - S_N p_N - bv - F_{ext}) \tag{21}$$

and $f(y,v,p_P,p_N) = k\left[\frac{S_p^2\left(\varphi(p_P) - \frac{S_P}{rT_c}p_P v\right)V_p(y) - S_p^3 p_P v}{V_p^2(y)} + \frac{S_N^2\left(\varphi(p_N) + \frac{S_N}{rT_c}p_N v\right)V_N(y) + S_N^3 p_N v}{V_N^2(y)}\right]$ (22)

Because of the modeling uncertainties, it is then necessary to close loop the system, and the classic feedback laws given by equation (23) are then used to stabilize the system (figure 6):

$$\begin{cases} w_1 = \frac{dK^d}{dt} - \lambda_K(K - K^d) \\ w_2 = j^d - \lambda_y(y - y^d) - \lambda_v(v - v^d) - \lambda_a(a - a^d) \end{cases} \tag{23}$$

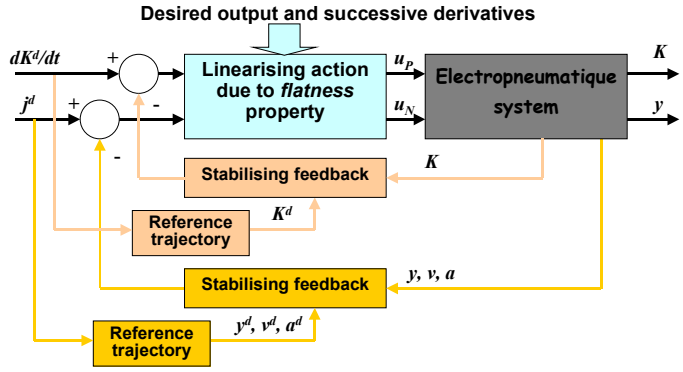

Figure 6: Flat system linearization and stabilising feedback

6 – Simulation results

The following results give an illustration of the overall control performance. The desired trajectories are been carefully chosen in order to respect the differentiability required by the model inversion although they will not fulfil the requirement of the physical system. The position trajectory is three times differentiable and define a stroke and back of the load. Two cases are shown concerning the stiffness trajectory: in the first case (figure 7), it is constant that is infinitely differentiable and in the second case (figure 8), the stiffness is parabolic when the load is moving and is then only once differentiable. The used model of the physical system for the simulation results is as realistic as possible and is evidently not the model used for mathematical inversion and control synthesis. The simulation model includes:

- a non linear sophisticated friction model including dry and viscous friction,
- a thermal model with cylinder convection as described in section 3,
- the servovalves measured static characteristics (different from polynomial approximation),
- the servovalves dynamics, identified from test rig.
- sensors models (quantification) and control loop sampling rate.

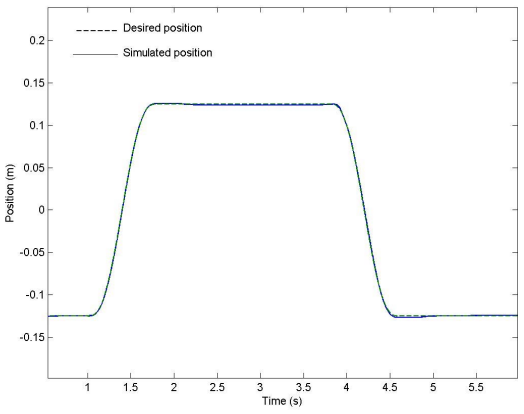

a) Position tracking

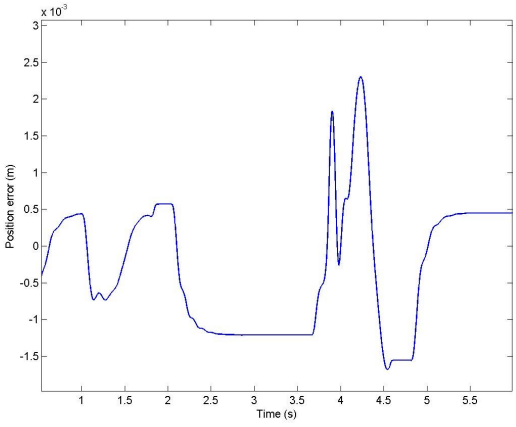

b) Position tracking error

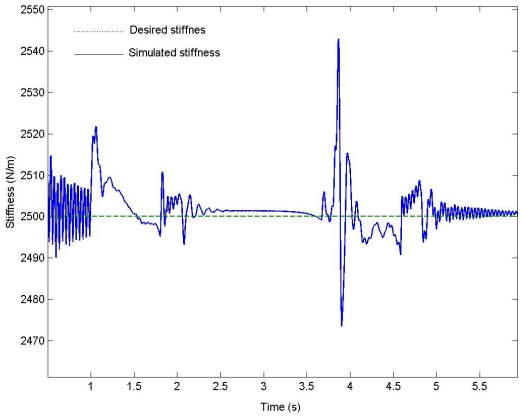

c) Stiffness tracking

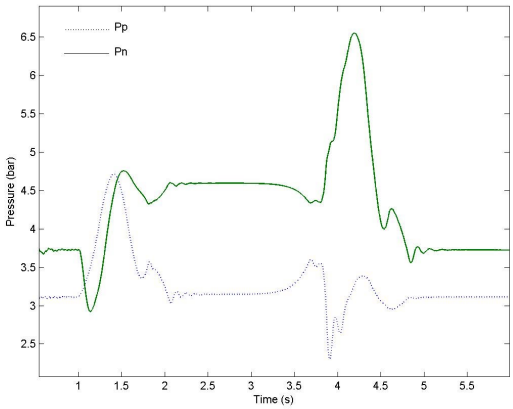

d) Pressure evolution

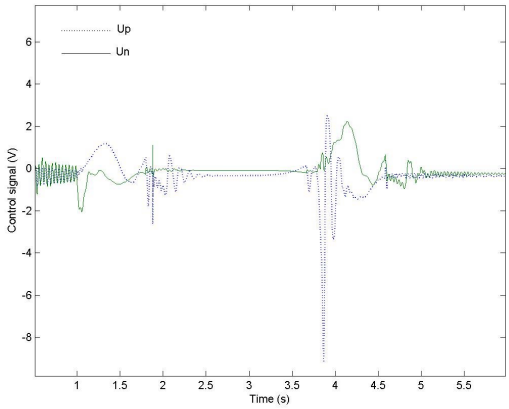

d) Inputs evolution

Figure 7: Desired and simulated results in the case of a constant stiffness

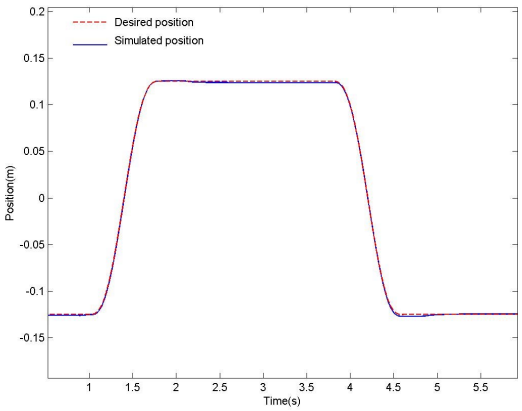

a) Position tracking

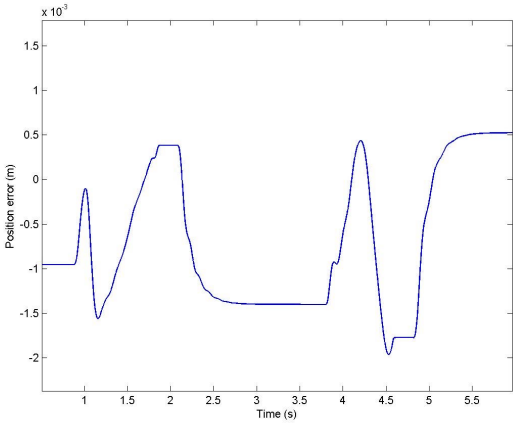

b) Position tracking error

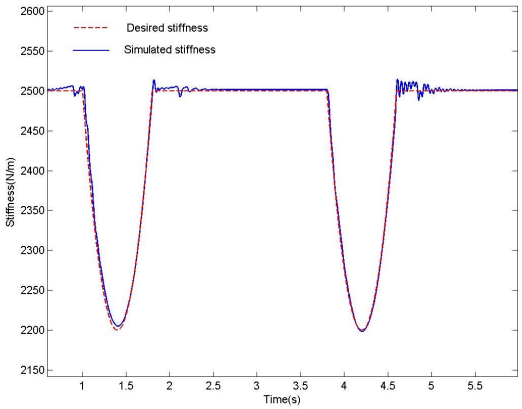

c) Stiffness tracking

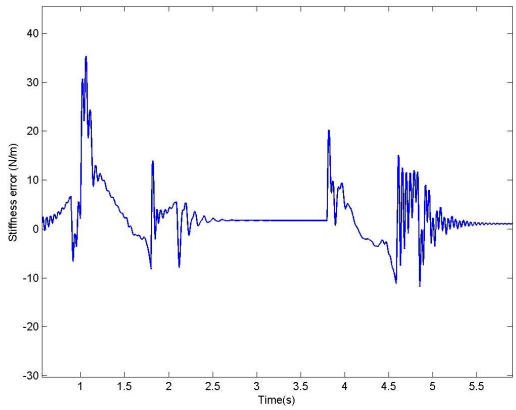

d) Stiffness tracking error

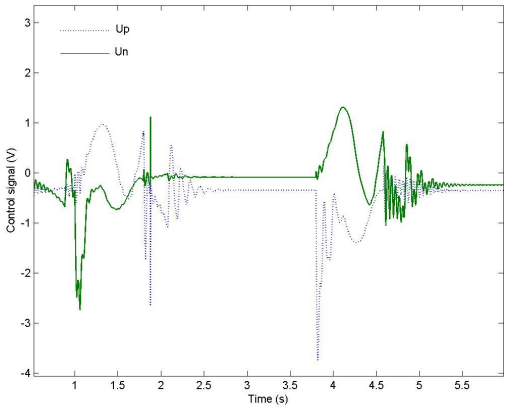

e) Inputs evolution

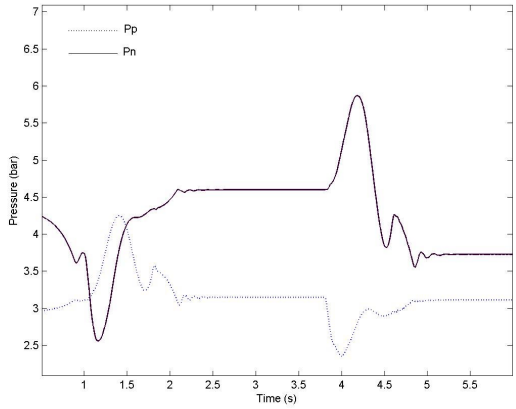

f) Pressure evolution

Figure 8: Desired and simulated results in the case of a parabolic stiffness

In all cases, the pressures and the input voltages evolve in the physical domain as the pressures are limited by the exhaust pressure (1 bar) and the supply pressure (7 bar), and the input voltage is saturated at ±10V. In the two cases, the position tracking error is less than 2.5 mm and the stiffness tracking error is no more than 45 N/m. Notice that in steady state, the errors are less than 1.2 mm in position and than 2 N/m in stiffness.

The position and stiffness errors occur when the movement starts and stops or when the stiffness changes. This can be explained by the approximation done for the model inversion and the uncertainties on the real system parameters (servovalves characteristics, friction, thermal behaviour, etc). Moreover it has been shown in section 4 that the model inversion requires differentiating the dry friction model. The behaviour around zero velocity constitutes the main difficulty that dry friction models try to solve because of the high variation of the friction force. This remark implies that physically there is a stiff gradient of the friction force when the spool leave or reach the steady state, which introduces errors in tracking and justify the necessity of more sophisticated feedback (18, 19).

7 – Conclusion

Firstly, it has been shown that it is important to take into account the control specification at the first of the system design (20), as the defined structure may have crucial effects on the reachable performance. Secondly, the proposed methodology for system inversion based on Bond graph presents many advantages as the structural inversion may be determined graphically and as it provides also a way to check the mathematical inversibility and flatness property of a system, the physical limitations or right choices and finally the inverse model which can be directly used in the control synthesis. Finally, the results show that even if the model is very realistic, the open loop control based on the system inversion has to be careful used because modelling uncertainties may have crucial effects as instabilities.

The proposed approach was applied for position and stiffness tracking in the case of a pneumatic cylinder but it can be exploited for other technologies as hydraulic, electrical actuators or hybrid drives, and using other outputs. Concerning this last remark, it appears clearly by the use of stiffness that the outputs are not necessary 'natural' outputs but can be combination of system states as energy consumption for example. The difficulty remains in defining the right output: physical or not. Future work will focus on the experimental implementation of this new approach.

REFERENCES

1. Brun, X., Thomasset, D., Sesmat, & S., Scavarda, S., "Limited energy consumption in positioning control of electropneumatic actuator", Power Transmission & Motion Control, Bath, UK, Sept. 1999, pp 199-211.
2. Gawthrop, P.J., "Bicausal bond graphs", International Conference on Bond graph Modeling and Simulation (ICBGM'95), January 15-18, 1995, Las Vegas, USA, Vol.27, n°1, p. 83-88.
3. Karnopp, D.C., Margolis, D.L. and Rosenberg, R.C., "System Dynamics – Modeling and Simulation of Mechatronic Systems", Third Edition, New York: John Wiley & Sons, Inc., 2000. 507 p.
4. Cornet A., Lorenz F., "Equation Ordering Using Bond Graph Causality Analysis", 12th IMACS World Congress, 1988, Vol. 1, Paris, pp. 43-46.
5. Ngwompo, R. and Gawthrop P., "Bond graph based simulation of nonlinear inverse systems using physical performance specifications", Journal of the Franklin Institute, 336(8):1225-1247, November 1999.
6. Ngwompo, R. F., Scavarda, S. and Thomasset, D., "Physical model-based inversion in control systems design using bond graph representation Part 1: theory", Journal of Systems, 2001, p. 95-103
7. Ngwompo, R. F., Scavarda, S. and Thomasset, D., "Physical model-based inversion in control systems design using bond graph representation Part 2: applications", Journal of Systems, 2001, p. 105-112
8. Gawthrop, P.J., "Control system configuration : Inversion and bicausal Bond graph", 3rd International Conference on Bond graph Modeling and Simulation (ICBGM'97), Jan. 1997, Phoenix, USA, p. 97-102.
9. Ngwompo, R., Scavarda, S. and Thomasset, D., "Inversion of linear time-invariant SISO systems modeled by bond graph", Journal of the Franklin Institute, 1996, p. 157-174, Vol. 333B n°2, March
10. Ngwompo, R., Scavarda, S. and Thomasset, D., "Structural inversibility and minimal inversion of multiavriable linear systems-a bond graph approach", International Conference on Bond graph Modeling and Simulation (ICBGM'97), January 12-15, 1997, Phoenix, Arizona, USA, Vol.29, n°1, p. 109-114.
11. E. Bideaux D. Martin de Argenta W. Marquis-Favre S. Scavarda, "Applying Causality and Bycausality to Mulit-Port Elements in Bond graphs", ", International Conference on Bond graph Modeling and Simulation (ICBGM'01), January 7-11, 2001, Phoenix, Arizona, USA.
12. Derkaoui, A., Bideaux E., Scavarda, S., "A First Approach Of Distributed Parameters Systems Sizing Using Bond graphs", Proceedings of the International Conference on Bond graph Modelling and Simulation (ICBGM'03), January,2003,Orlando, USA, Vol.35, n°1, pp. 79-86.
13. Fliess, M., Levine, J., Martin, P., & Rouchon, "P. Flatness and defect of non-linear systems : introductory, theory and applications", International Journal of Control, 1995, Vol. 61, pp. 1327-1361.
14. Isidori, A., "Nonlinear control systems", New York : Springer Verlag, 2nd edition, 1989, 479 p.
15. Shearer, J.L., "Study of pneumatic processes in the continuous control of motion with compressed air. Parts I and II", Trans. Am. Soc. Mech. Eng., 1956, **78**, 233-249.

16. Sesmat, S., Scavarda, S., Lin-Shi, X., "Verification of electropneumatic servovalve size using non-linear control theory applied to a cylinder position tracking", 4th Scandinavian International Conference on Fluid Power, SICFP'95, Tampere, Finland, Sept. 95, Vol.1, pp. 504-513.
17. Belgharbi, M., Thomasset, D., Scavarda, S., & Sesmat, S., "Analytical model of the flow stage of a pneumatic servo-distributor for simulation and nonlinear control", 6th Scandina. Int. Conf. on Fluid Power, SICFP'99, Sept. 99, Tampere, Finland, Vol.2, pp. 847-860.
18. Richard, E., Scavarda, S., "Comparison between Linear and Nonlinear control of an eletropneumatic servodrive." Jour. of Dynamic System Measurement & Control, June 1996, Vol. 118, p 245-252.
19. Brun X., Belgharbi M., Sesmat S., Thomasset D., Scavarda S., "Control of an electropneumatic actuator, comparison between some linear and nonlinear control laws", Journal of System and Control Engineering, 1999, Vol. 213, N°I5, pp. 387-406.
20. Brun, X., Thomasset, D., Bideaux, E., "Influence of the process design on the control strategy: application in electropneumatic field", Control Engineering Practice, Volume 10, Issue 7, July 2002, Pages 727-735.